JOURNAL OF SOLID STATE CHEMISTRY **128,** 109–114 (1997)
ARTICLE NO. SC967181

The Magnetic Structure of Ordered Cubic Pd_3Mn

Per Önnerud, Yvonne Andersson, and Roland Tellgren

Institute of Chemistry, Uppsala University, Box 531, S-751 21 Uppsala, Sweden

and

Per Nordblad

Department of Technology, Uppsala University, Box 534, S-751 21 Uppsala, Sweden

Received August 7, 1996; accepted October 3, 1996

Neutron powder diffraction and magnetization measurements have been carried out on ordered cubic Pd_3Mn of the Cu_3Au-type structure. The crystal and magnetic structures have been analyzed by means of the Rietveld method. The magnetic structure model was refined to a modulated incommensurate helical cone structure with a propagation vector along the crystallographic (111) direction. The obtained magnitude of the moments was 5.0 μ_B per manganese atom at 10 K.

I. INTRODUCTION

Pd_3Mn crystallizes in a disordered fcc-type structure above a critical temperature of 800 K. This phase is known to exhibit spin-glass behavior (1) and was recently examined by Saha *et al.* who reported on magnetic properties of disordered fcc Pd-Mn alloys (2). Below 800 K the compound slowly orders to a tetragonal structure of the Al_3Zr-type (3). Flanagan and co-workers have shown that a hydrogen induced order–disorder transition of the compound from the tetragonal phase to an ordered cubic structure of the Cu_3Au-type, space group $Pm3m$, occurs when applying a hydrogen pressure of 5 MPa at a temperature of 523 K (4). The cubic phase is metastable in air with a very slow decomposition time at room temperature.

Different groups have reported on the magnetic structures of tetragonal Pd_3Mn [3, 5, 6], which is a collinear antiferromagnet with the magnetic moments pointing mainly along the c-axis. All studies agree that the size of the magnetic moment of the manganese atoms is around 4.5 μ_B/atom with some variation with temperature. A small magnetic moment on the Pd atoms (< 0.2 μ_B/atom) has also been reported. Krén and Kádár found that the direction of the magnetic moment changes with composition of Pd and Mn with the moments tilted at an angle 8(2)° from the c-axis for the 3 : 1 composition. Rodic *et al.* have confirmed this by reporting a tilt angle of 11(1)° for the same composition. The Néel temperatures do however vary between 170 and 200 K in the different investigations.

Men'shikov and co-workers have studied atomic and magnetic structures of the $Pd_3(Fe_{1-x}Mn_x)$ system (7). Pd_3Fe crystallizes in the Cu_3Au-type (Ll_2) structure and a ferromagnetic behavior was reported for $x < 0.6$. Substitution with Mn for Fe in the composition range $0.6 < x < 1$ makes the compound form a tetragonal phase with an antiferromagnetic behavior.

Magnetic ordering of cubic Pd_3Mn has been predicted by Jaswal (8), from theoretical calculations, using the orthogonalized linear combination of atomic orbitals (OLCAO) method. Ordering was also theoretically predicted by Nautiyal *et al.* (9) who have performed self-consistent band calculations using the linear-muffin-tin-orbital (LMTO) method.

In this paper we report on a magnetic structure investigation on ordered cubic Pd_3Mn by means of magnetization and neutron powder diffraction measurements.

2. EXPERIMENTAL

A. Sample Preparation

The alloy was prepared by high-frequency melting from the pure metals in an argon atmosphere. The product was then crushed and ground to a powder which was heated in vacuum at 740 K for 24 h followed by slow cooling which made the sample order in a tetragonal structure. To obtain the cubic phase, the compound was annealed for one week at approximately 500 K in a hydrogen pressure of 5 MPa. A Guinier–Hägg focusing camera recorded X-ray photographs for phase analyses. The unit cell dimension $a = 3.9014(5)$ Å was determined at room temperature with silicon ($a = 5.431065$ Å) as internal standard. X-ray intensity data were collected with an STOE diffractometer using

0022-4596/97 $25.00

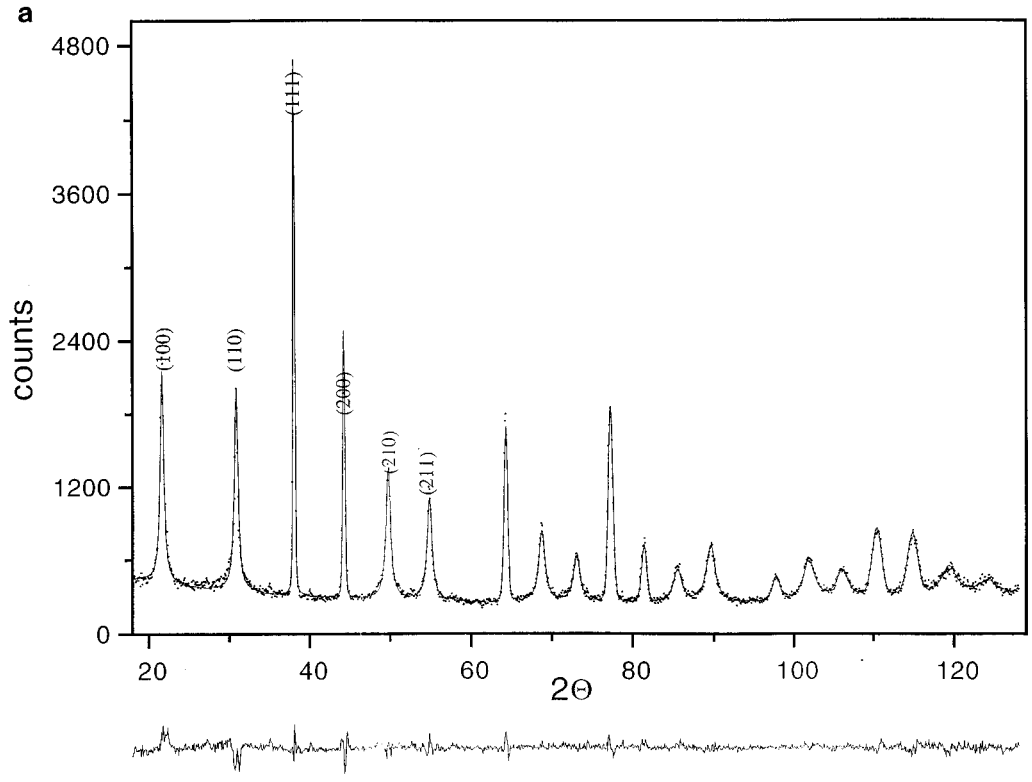

FIG. 1. Neutron powder diffractograms of Pd_3Mn at (a) 295 K and (b) 10 K. The calculated intensities are in full line, and the observed intensities are dotted. The difference line is shown at the bottom of the figure.

a small position sensitive detector between 10 and 100° in 2θ. The radiation used in both X-ray cases was Cu$K\alpha_1$. The X-ray powder diffraction patterns showed in addition to the ordered cubic Pd_3Mn lines some very weak reflexions belonging to tetragonal Pd_3Mn. The total amount of the tetragonal phase was estimated to be less than 2 wt%. The total composition of the sample was also confirmed by chemical analysis.

B. Neutron Powder Diffraction Data Collection

The Neutron powder diffraction work was carried out at the Swedish R2 reactor in Studsvik. The neutron beam was monochromated from two copper (220) single crystals in a parallel arrangement giving a wavelength of 1.470(1) Å. Diffractograms were collected at 295 and 10 K and are shown in Fig. 1. The cryostat gave rise to an extra reflexion at $2\theta = 36.6°$. A detector bank of 10 detectors separated by 3.12° measured the intensities in steps of 0.08° in 2θ, within a scan-range of 0.2–128.04°. The contributions from the different detectors were statistically analysed and added. Absorption effects were corrected for by using the experimentally determined value $\mu R = 0.41$ from transmission measurements at $2\theta = 0°$.

3. DETERMINATION OF THE MAGNETIC STRUCTURE

A comparison of the diffractogram obtained at 10 K with that obtained at 295 K shows one additional strong reflexion in the low-angle area. The reflexion which is partly overlapped by the primary beam is centered at $2\theta = 3.65°$. Clearly visible satellite reflexions can also be seen on both sides of the (001) and (011) peaks and small satellites are observed around the (111), (200), and (210) peaks, Fig. 1. These new peaks at 10 K were interpreted as Bragg reflexions originating from an ordering of the magnetic moments on the manganese atoms. An analysis of the satellites and the strong $\pm$ (000) peak indicate an incommensurate helical structure, with a modulated propagation vector along the [111] direction. In the Rietveld refinements calculated diffraction intensities based on this model resulted in good agreement with the observed intensities.

4. RIETVELD REFINEMENTS

The diffraction data were refined using the Rietveld method (10) implemented in the FULLPROF-program by Rodriguez-Carvajal (11). As seen in Fig. 1 the diffraction peaks of the fundamental lines having *hkl* all odd or all even

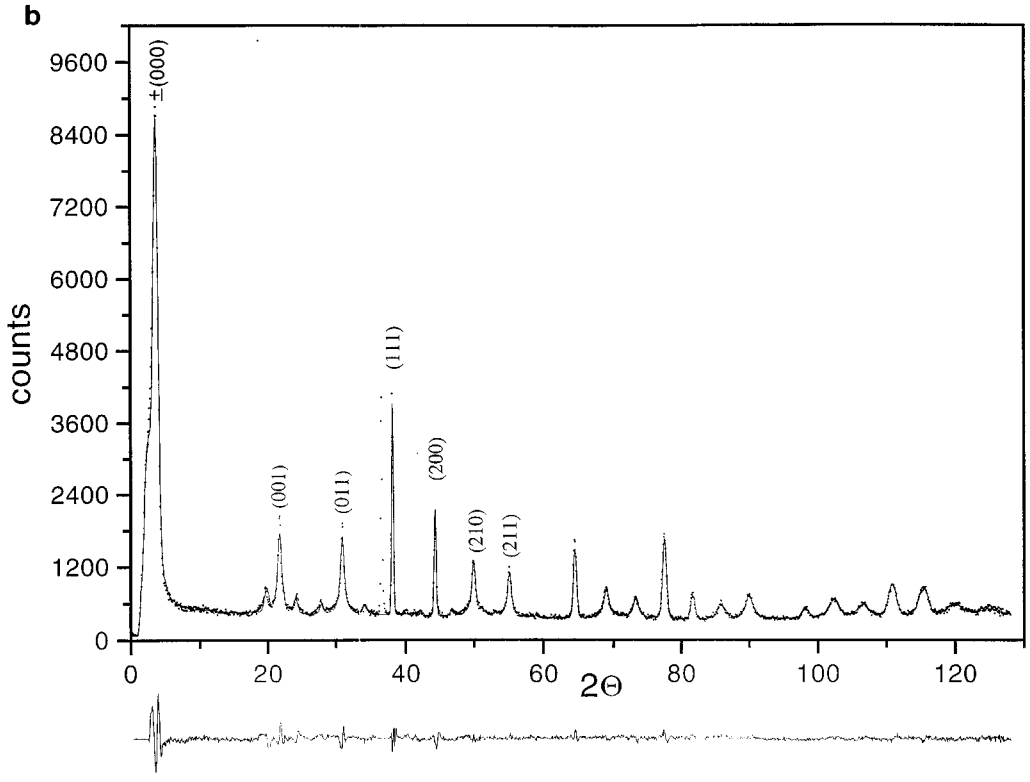

FIG. 1—*Continued.*

are much more narrow than the superlattice peaks with mixed *hkl*. This is due to anti-phase domains and was taken care of in the refinements by using different *hkl* lists with different peak shape and half-width parameters, *U*, *V*, and *W*. The superlattice peaks were refined as Lorentzian, while the peak shape of the fundamental reflexions had only a small Lorentzian contribution to an almost pure Gaussian peak shape. To refine the disorder of manganese atoms in the palladium site and vice versa, a coupled parameter for the two atoms was used in the 295 K data set. The refined distribution from the 295 K data set was later used as constant values in the low temperature refinement. The neutron diffraction technique is very well suited to clarify the disorder problem as the scattering for manganese is

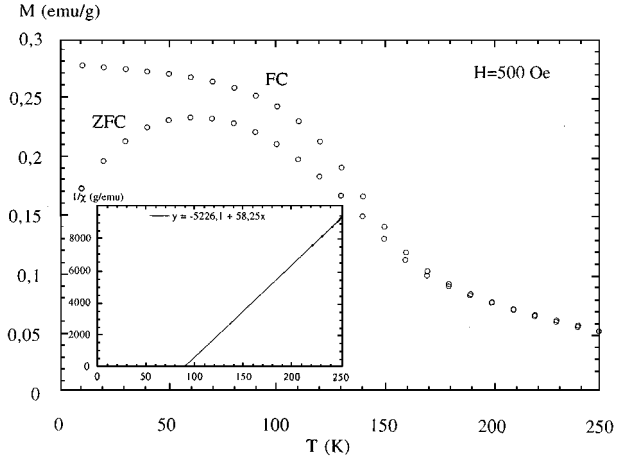

FIG. 2. Magnetization vs temperature for Pd_3Mn (cubic). Zero field cooled (ZFC) and field cooled (FC) curves are shown. The inset shows a fit of the high-temperature part to Curie–Weiss behavior.

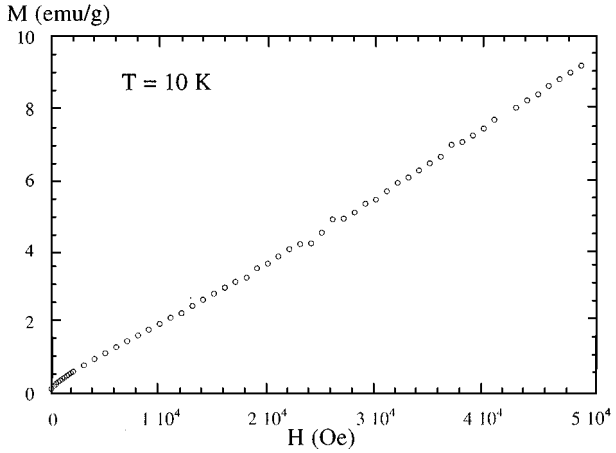

FIG. 3. Magnetization vs field for Pd_3Mn (cubic) at 10 K.

negative, ($b_{Mn} = -3.73$ fm) compared to palladium which has a positive scattering length of $b_{Pd} = 5.91$ fm. This means that the intensities of the peaks having mixed *hkl* will be enhanced compared to the X-ray case where these peaks are very weak. Additionally one scale factor, one zero point, and one unit cell parameter were refined. One isotropic thermal parameter was refined for each crystallographic site. The background intensities were in the 295 K data set described by a polynomial expression $y_i = \sum B_m(2\theta_i/90 - 1)^m$, where $0 < m < 5$. All six B_m coefficients were varied. In order to describe the (000) reflexion, in the 10 K data set, the background was described by interpolating linearly between 55 background points. In the 295 K data set the region of the diffractogram belonging to the primary beam was cut off. Two additional parameters were included in order to refine the fourier components of the magnetic moments. One parameter was describing the helix and the other representing an additional ferromagnetic contribution to the magnetic moment. Altogether 19 parameters were refined for the diffractogram recorded at 295 K and 16 parameters were used for the 10 K data set.

5. MAGNETIZATION MEASUREMENTS

The magnetization measurements were performed on a Quantum Design MPMS SQUID-magnetometer system utilizing a 5.5 T super conducting magnet to provide an external field. Both magnetization (M) versus temperature in a constant applied field (H) Fig. 2 and M versus H curves at constant temperature were recorded, Fig. 3.

As can be seen in Fig. 2 the magnetization curve shows a magnetic transition at a critical temperature of $\sim$190 K. From the slope of the curve in the inset of Fig. 2 p_{eff} was calculated to 7.2 μ_B/Mn and can be compared with values calculated from p_{eff} by Saha *et al.* (2) which gives $p_{eff} = 7.2\ \mu_B$/Mn for the 3:1 composition. However, it should be noted that the p_{eff} values in ref. (1, 2) are wrongly calculated. In the formula $p_{eff} = \sqrt{3Ck_B/N/\mu_B}$ the authors have used N as Avogadro's number. N should be the number of atoms in 1 g of the compound since the Curie constant C is given in the unit (10^{-3} emu/gOe)K, (k_B is the Boltzmann constant and μ_B the Bohr magneton). The correct p_{eff} value for the 3:1 composition should be 7.3 μ_B/Mn and in Table 1 the recalculated p_{eff} values from ref. (1, 2) are tabulated. As seen from the magnetization measurements at 10 K, there is no tendency toward saturation of the sample. Although a field of 5 T is used, the magnetization does not deviate much from a linear dependence on the applied field at higher fields. There is a closely linear M vs H dependence in the high-field region of the magnetization curves. The linear increase corresponds to $M/H \sim 2 \times 10^{-4}$ emu/g giving a magnetization of $\sim$0.7 μ_B/Mn at 5 T.

TABLE 1
Recalculated p_{eff} Values for Disordered $Pd_{1-x}Mn_x$ from References [1, 2], cf. Comments in Ch. 5.

x in $Pd_{1-x}Mn_x$	p_{eff} (μ_B/fu)	p_{eff} (μ_B/Mn)
0.020	1.4	10.2
0.040	1.6	8.2
0.094	2.4	7.9
0.147	2.4	6.2
0.184	2.4	5.5
0.200	2.5	5.7
0.222	2.5	5.4
0.244	3.4	6.9
0.250	3.7	7.3

6. RESULTS AND DISCUSSION

The proposed model with the magnetic moments of the manganese atoms forming a helical cone structure was confirmed by the Rietveld refinements. Structure parameters are listed in Table 2 together with agreement factors. In order to measure the magnetic transition temperature the $\pm$(000) peak was scanned at 12 different temperatures. The

TABLE 2
Parameters from the Rietveld Refinement

T	a [Å]	occ. (Pd)	occ. (Mn)	B_{Pd} (Å^2)	B_{Mn} (Å)	R_P	R_B	R_M
295 K	3.8991 (2)	0.981 (6)	0.943 (6)	0.58 (4)	0.3 (1)	5.25	2.64[1] 1.62[2]	— —
10 K	3.8877 (3)	0.981[a]	0.943[a]	0.43 (4)	0.19 (8)	5.35	6.17[1] 4.07[2]	3.90[3], 4.63[4] 3.76[5]

Note. 1–5 show the R-values of the crystalline and magnetic components as they occur in the refinement. 1 and 2 belongs to the crystalline phase. 3 is the helix magnetic parts and 4, 5 are the ferromagnetic parts. 1 and 4 have R-values corresponding to all *hkl* odd or even; 2 and 5 have mixed *hkl*'s.

[a] The parameter is kept constant during the refinement.

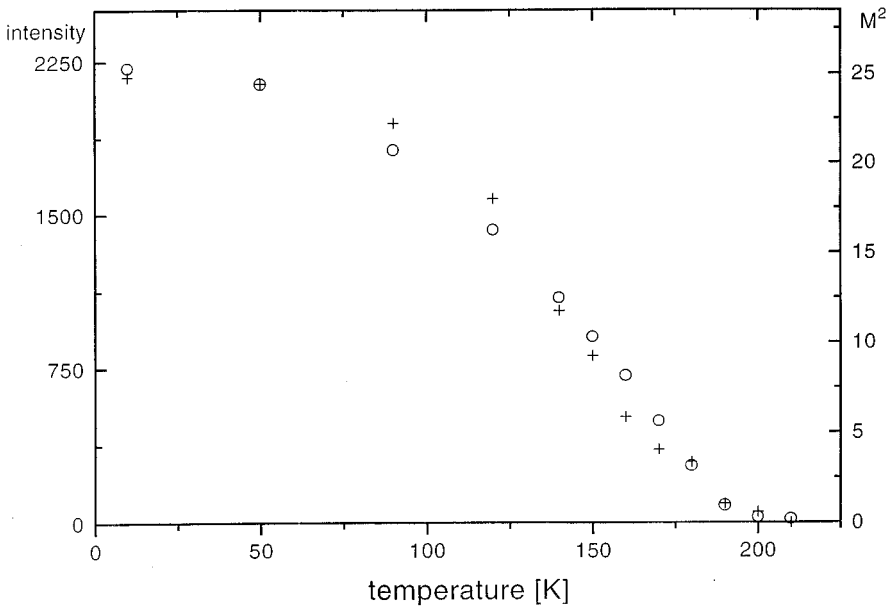

FIG. 4. Intensity of the $\pm$ (000) peak (crosses) and a calculated Brillouin curve (circles) of the magnetization as a function of temperature.

Brillouin behavior of the intensity as a function of temperature of the first magnetic reflexion is plotted and compared with a calculated Brillouin curve, Fig. 4, showing the transition temperature to be 190 ± 5 K. The calculated Brillouin curve was obtained using $S = 5/2$ and $T_c = 190$ K (12). The propagation vector was refined to [0.0972(4), 0.0972(4), 0.0972(4)] which gives a modulated helix axes of length 23.1 Å in the [111] direction and a rotation angle of the spins of 35.0(2)° for successive magnetic sheets projected on the [111] planes. The neutron diffraction refinement on 10 K data yields a moment of $2.9(1)\mu_B$ per manganese atom for the ferromagnetic part and the helical component of the moment was refined to 4.11(4) μ_B. In our model the refined values above would correspond to a total magnetic moment of 5.0 μ_B per manganese atom with the moments forming an angle of $\sim 55°$ with the helix axes. Attempts were made to refine magnetic moments belonging to the palladium atoms but as in the tetragonal phase no significant moment could be determined. The total magnetic moment obtained is in good agreement with results from Rodic *et al.* (3). In tetragonal Pd_3Mn a moment of 5.2(1) μ_B at 10 K and 4.7(1) μ_B at 70 K was observed on the manganese atoms. Compared to the isostructural Pd_3Fe the moments are also of the same order, this phase has been reported to have an effective moment of 4.8 μ_B/fu. The results from magnetization measurements using the Curie–Weiss law give comparable values of the magnetic moments. The derived magnetic structure is shown in Fig. 5.

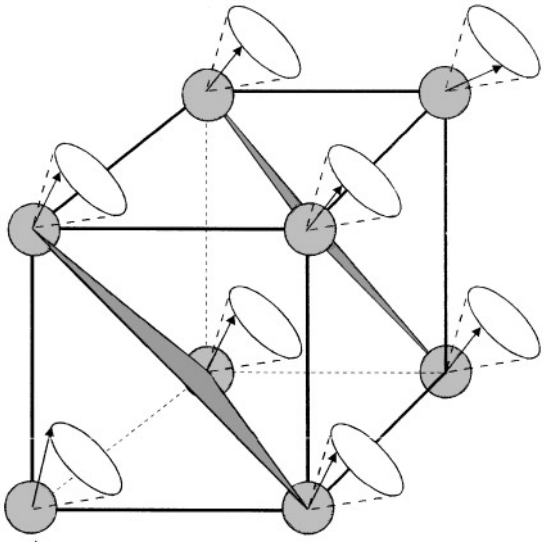

FIG. 5. The magnetic helical cone structure of cubic Pd_3Mn. For clarity only the manganese atoms are shown in the structure.

ACKNOWLEDGMENTS

We are indebted to H. Rundlöf for skillful assistance during neutron data collection. Thanks are also due to the Swedish Natural Science Research Council (NFR) for financial support.

REFERENCES

1. M. H. Rashid and D. J. Sellmyer, *J. Appl. Phys.* **55** (6), 1735 (1984).
2. D. K. Saha, K. Ohshima, M. Y. Wey, R. Miida, and T. Kimoto, *Phys. Rev.* **B49,** 15715 (1994).
3. D. Rodic, P.-J. Ahlzén, Y. Andersson, R. Tellgren, and F. Bouree-Vigneron, *Solid State Commun.* **78** (8), 767 (1991).
4. T. B. Flanagan, A. P. Craft, T. Kuji, K. Baba, and Y. Sakamoto, *Scr. Metall.* **20,** 1745 (1986).
5. J. W. Cable, E. O. Wollan, W. C. Koehler, and H. R. Child, *Phys. Rev.* **128,** 2118 (1962).
6. E. Krén and G. Kádár, *Phys. Lett.* **29,** 340 (1969).
7. S. G. Bogdanov, A. Z. Men'shikov, and Y. A. Vereshchagin, *Fiz. Met. Metalloved.* **66,** 404 (1988).
8. S. S. Jaswal, *Solid State Commun.* **52,** 127 (1984).
9. T. Nautiyal and S. Auluck, *J. Phys.: Condens. Mat.* **1,** 2211 (1989).
10. H. M. Rietveld, *J. Appl. Crystallogr.* **2,** 65 (1969).
11. J. Rodriguez-Carjaval, ILL Internal Report, FULLPROF Computer Program.
12. D. F. Martin, "Magnetism in Solids," p. 223. Iliffe Books Ltd, London, 1967.